J Clin Res Paramed Sci. 2021 December; 10(2):e119150. https://doi.org/10.5812/jcrps.119150.

Published online 2021 December 10. **Research Article**

Thin TiO_2 Nanocoating of Porous Titanium through Radio Frequency Magnetron Sputtering to Improve the Biological Response of Orthopedic Implants

Roghayeh Haghjoo [1], Seyed Khatiboleslam Sadrnezhaad [2,*] and Nahid Hassanzadeh Nemati [1]

[1] Department of Biomedical Engineering, Science and Research Branch, Islamic Azad University, Tehran, Iran
[2] Department of Materials Sciences, Sharif University of Technology, Tehran, Iran

[*] *Corresponding author*: Department of Materials Sciences, Sharif University of Technology, Tehran, Iran. Email: sadrnezh@sharif.edu

Received 2021 August 29; **Revised** 2021 November 23; **Accepted** 2021 November 27.

Abstract

The present study applied a TiO_2 nanocoating on a titanium foam substrate produced by powder metallurgy through magnetron sputtering. Scanning electron microscopy (SEM), energy-dispersive X-ray spectroscopy (EDS), and X-ray diffraction (XRD) were employed to investigate the surface morphologies of the porous specimens and pre- and post-coating phases, respectively. Also, the growth and proliferation of MG-63 cells (osteoblasts) and their attachment and proliferation on the coated porous titanium specimen (relative to the uncoated specimens) were studied using in vitro and methyl thiazol tetrazolium (MTT) cytotoxicity tests. Considering the porous macrostructure of the coated titanium specimen and the nanostructure of the TiO_2 coating on the porous surface and macro-pore walls, the coated specimen was found to be effective in the biocompatibility improvement of dental and orthopedic implants.

Keywords: Cellular Behavior, Implant, Nanocoating, Magnetron Sputtering, Thin Layer, Titanium Foam

1. Background

Since they can resist high loads, metals are employed in dental and orthopedic implants. Due to its high corrosion resistance in the body environment, relatively low elasticity modulus, suitable fracture toughness, and a large strength-to-density, titanium is widely employed in medical applications (1). However, such implants deteriorate due to their long fixation time, which deprives the bony socket of loading for a long time. Moreover, since titanium has a higher density and rigidity than the bone, a harmful load is applied by the implant to the bone, leading to the loosening or fracture of the implant (2, 3). Researchers have developed several porous metals, such as titanium foams, for orthopedic implant applications (4). Porous metals are a new group of materials with unique properties, such as low density, high strength-to-weight ratios, large specific area, and excellent energy absorption (5). New porous metals enable bone cells to growth within pores, improving fixation and accelerating healing (6, 7). The strength and elasticity modulus of a porous metal-produced implant can be adjusted based on the target area (8). Thus, porous metals are a suitable alternative to restore or replace damaged bones due to their excellent biocompatibility and similar stiffness to the bone required for dental and orthopedic replacement applications (9).

Nanostructures control the fate of cells and have been of great interest to researchers for the improvement of surface characteristics in the host-implant interface (10). From this perspective, the application of a nanostructure on the implant surface increases the interaction of serum proteins. This may be an appealing strategy to promote the bone conduction and induction characteristics of an implant. Although this factor is typically overlooked in implants, it could play a key role in obtaining desirable bone functions (11). To improve the properties of the surface in contact with living tissues, metals used in medical implants require surface treatment (12). The biological characteristics of implant surfaces could be improved by adding materials of desirable properties, changing the composition, or removing undesirable materials from the implant surface (13, 14). Since titanium can form an oxide layer on its surface (as with other transition metals), a thin, regular, and nanostructured oxide layer can be grown on the surface of a titanium implant using a number of techniques, such as plasma spraying, electrostatic spraying, pulsed laser, micro-arc oxidation (MRO), sol-gel depo-

sition, and magnetron sputtering (15). Magnetron sputtering is an ideal titanium coating technique to create a thin nanostructured biocompatible TiO_2 layer. A thin TiO_2 layer with a desirable nanostructure could be created by selecting proper deposition parameters (13, 16)

2. Objectives

Many studies have been conducted on the formation of a thin TiO_2 layer on a titanium substrate using various techniques. However, thin nanostructured TiO_2 layer formation on a porous titanium substrate has not been reported. The present study fabricates porous titanium specimens using powder metallurgy. Then, the porous substrate is coated with a thin nanostructured TiO_2 layer through magnetron sputtering to explore the effects of the TiO_2 nanocoating of titanium foam on its biological characteristics.

3. Methods

3.1. Fabrication of Specimens

This study was conducted in two stages: (1) fabricating porous titanium specimens by the powder metallurgy-space holder process and (2) coating the porous titanium specimens (i.e., titanium foams) by magnetron sputtering. Titanium powder (average particle size of 45 μm, produced by Merck) and an acicular space holder (urea, an average particle size of 500 - 800 μm, produced by Merck) were mixed at a pore volume fraction of nearly 50% to fabricate porous specimens. Then, the metal powder-space holder mixture was pressed at nearly 120 MPa within a cylindrical steel mold (8 mm of diameter) by a uniaxial hydraulic cold pressing machine (Khavaran Press Co.). The specimens were heat-treated using a YTF 1800-30X8H tube furnace (Yaran Behgozin Parsa Co.) under vacuum at 2×10^{-5} Torr to avoid oxidation. Since the powder urea space holder would evaporate at nearly 176°C, heat treatment to remove the space holder was implemented at 200°C at a rate of 5°C/min to avoid the abrupt removal of the space holder and damage to the porous structure. The specimens were kept at 200°C for 45 min to ensure the complete removal of the space holder. Heating was performed from 200°C to 1000°C at a rate of 10°C/min for 1 h. Finally, the specimens were kept at 1000°C for 2 h to ensure complete sintering. To obtain a smooth surface for a uniform coating, the porous titanium specimens were polished using 600 - 2000 sandpaper. Then, they were degreased in an ethanol-acetone bath, rewashed with distilled water, and dried.

To apply a nanostructured TiO_2 coating on the specimen surface, a hollow pure titanium cylinder (Yarnikan Saleh Co.) was placed in the magnetron sputtering machine (Yarnikan Saleh Co.). The TiO_2 coating was applied to the titanium foam substrate at a DC of 200 mA. The sputtering of the specimens was performed at a basic pressure of 5×10^{-5} Torr by applying a DC and a 90:10 atmosphere of argon and oxygen at the operating pressure of 2×10^{-5} Torr for 30 min. The Ti atoms were removed from the target surface by the ionized gases and oxidized by reacting to the O atoms in the atmosphere while depositing. Thus, a TiO_2 layer formed on the substrate.

To improve the attachment and uniformity of the coating, the specimens were subjected to heat treatment at 480°C for 2 h. To avoid thermal stress in the coating, a slow heating rate of 2°C/min was applied to the secondary heat treatment.

3.2. Morphology Evaluation

Scanning electron microscopy (SEM) were employed to examine the pore geometry, coating microstructure, and cell growth on the specimens before and after coating. The MIRA 3-XMU SEM machine manufactured by TESCAN Co. was used.

To obtain high-resolution SEM images, a thin Au layer was deposited onto the specimens using the sputtering machine to provide a better current.

3.3. Phase Structure Characterizations

To investigate the phases, X-ray diffraction (XRD) was employed (EQUINOX 3000 machine, Intel Corporation, France). The XRD test was carried out at a 2θ of 20 - 80° and a scanning rate of 0.02°/s. The tube provided copper Kα beams with a wavelength of 1.54 Å. The XRD patterns were plotted and analyzed using X'Pert HighScore Plus.

To evaluate the distribution of elements across the specimens and the elements and compounds of the nanocoating, the energy-dispersive spectroscope (EDS) detector on the SEM was employed.

3.4. In vitro Studies

3.4.1. Cell Culture

To determine cytotoxicity, cell proliferation, and cell morphologies, MG-63 osteoblasts (NCBI C 555) were obtained from the cell bank of the Pasteur Institute of Iran. Since the cylindrical specimens had a diameter of 8 mm and a height of 5 mm, a cell culture plate with 24 wells was employed. Dulbecco's Modified Eagle's Medium (DMEM) was used for cell culture (GIBCO Corporation, Scotland), to which 10% of fetal bovine serum (FBS) (Seromed Co, Germany) along with 100 IU/mL of penicillin and 100 μg/mL of streptomycin (Sigma Co., USA) were added. First, 1 mL of the culture medium was poured into the wells. Then, the

porous titanium specimens (the coated porous and control specimens) were placed in the medium. Once the complete submersion of the specimens in the culture medium and the proper placement of the specimens (to cover the maximum area on the bottom of the well) had been ensured, a total of 10^4 cells with 1 mL of the prepared culture medium were added to the wells. A well with no specimen and the same number of cells was used for negative control. The osteoblasts were cultured.

3.4.2. Cell Morphology

SEM was used to determine the morphology of the cultured cells on the titanium foams and nanostructured titanium specimens. The specimens with cells were placed in an incubator at 37°C with a CO_2 content of 5% and a relative humidity of 98%. Once the specimens and cells had been in contact for 24 h. Cells were stabilized using a 2.5% glutaraldehyde solution. The specimens were washed twice with a 0.2% molar phosphate-buffered saline (PBS) physiological serum. Then, each specimen was placed in a 2 mL glutaraldehyde solution for 2 h. The specimens were kept in 2 mL of ethanol solutions with a concentration of 40 - 95% for 5 min before they were placed in 100% alcohol for 10 min. The surface moisture of the specimens was measured in ambient conditions after dewatering.

3.4.3. Cell Survival and Proliferation

To evaluate the toxicity and proliferation of cells, extraction (indirect testing) was carried out. According to the ISO 10993-12 Standard, the extraction of the specimens was performed, in which 0.1 mL of the culture medium was added to the plate per 0.6 cm^2 of the specimen surface area. The specimens were placed within an incubator at a CO_2 concentration of 5% and a culture temperature of 37°C for 3 and 7 days. The same volume of the culture medium was used as the control measure.

The methyl thiazol tetrazolium (MTT) test was carried out to investigate cell proliferation. A total of 10^4 cells were poured into a cell culture plate with 96 cells. Then, it was kept in an incubator at 37°C for 24 h so that the cells would attach to the plate bottom. The extract of each specimen was added to the culture well, placing the cells in the vicinity of the extracts for 3 and 7 days. Then, the culture medium was removed, adding 100 μL of MTT to each well at a concentration of 0.5 mg/mL. After four hours, the solution on the cells was removed, adding isopropyl alcohol (Merck) to dissolve the violet crystals. Then, the concentration of the dissolved substance in the isopropyl alcohol solution was measured at a wavelength of 545 nm.

3.5. Statistical Analysis

Deviance analysis of data was utilized using analysis of variance (ANOVA). Statistical analysis was performed using SPSS. Differences and parameters were considered statistically at a significance level of $P < 0.05$.

4. Results and Discussion

4.1. Morphology and Microstructure

Figure 1 shows the SEM images of porous titanium fabricated by the space holder (urea). As mentioned, the space holder was acicular and had a size of 500 - 700 μm. The dark areas represent pores. As can be seen, the pore shapes were a function of the initial space holder shape. There are two types of pores: (1) open or interconnected macropores and (2) closed or discrete micropores. Macro-pores arose from the evaporation of the space holder and have an interconnected structure. The shape, size, and number of macropores are dependent on the shape, size, and quantity of the space holder (17). Urea decomposes into water, CO_2, and NH_3 when heated (18). The use of urea as the space holder increases the gas pressure, leading to trapped gas removal and open and interconnected pores (18).

As can be seen in Figure 2, a nanostructure formed on and within foam pores after sputtering. A thin deposited TiO_2 coating was deposited uniformly on the porous Ti substrate. The entire porous titanium substrate was coated, and even a continuous non-cracked coat formed within the substrate pores. It should be noted that the specimens cooled down at the plate temperature after deposition to avoid possible thermal stresses (13).

The titanium foam surface and the inner surface the pores represent a nanostructured TiO_2 coating. Considering the nanostructured rough surface, this topography can play a key role in the bioactive behavior of the titanium foam since surface roughness and porosity are essential properties that significantly influence the performance of implants (19). Pores are important in the sense that they affect the specific surface area in contact with the body environment and physicochemical interactions in the host-implant interface (15). Moreover, sufficient porosity on the surface transmits nutrients and metabolic substances, controls biological performance, and enables cell proliferation (12). As a result, the surface treatment and coating of implants are performed to create a porous, rough surface.

4.2. Energy-Dispersive X-Ray Spectroscopy Evaluation

Figure 3 depicts the energy-dispersive X-ray spectroscopy (EDS) results of porous titanium and the nanostructured TiO_2 coating on the porous titanium surface. As can be seen, no unwanted transmission element was

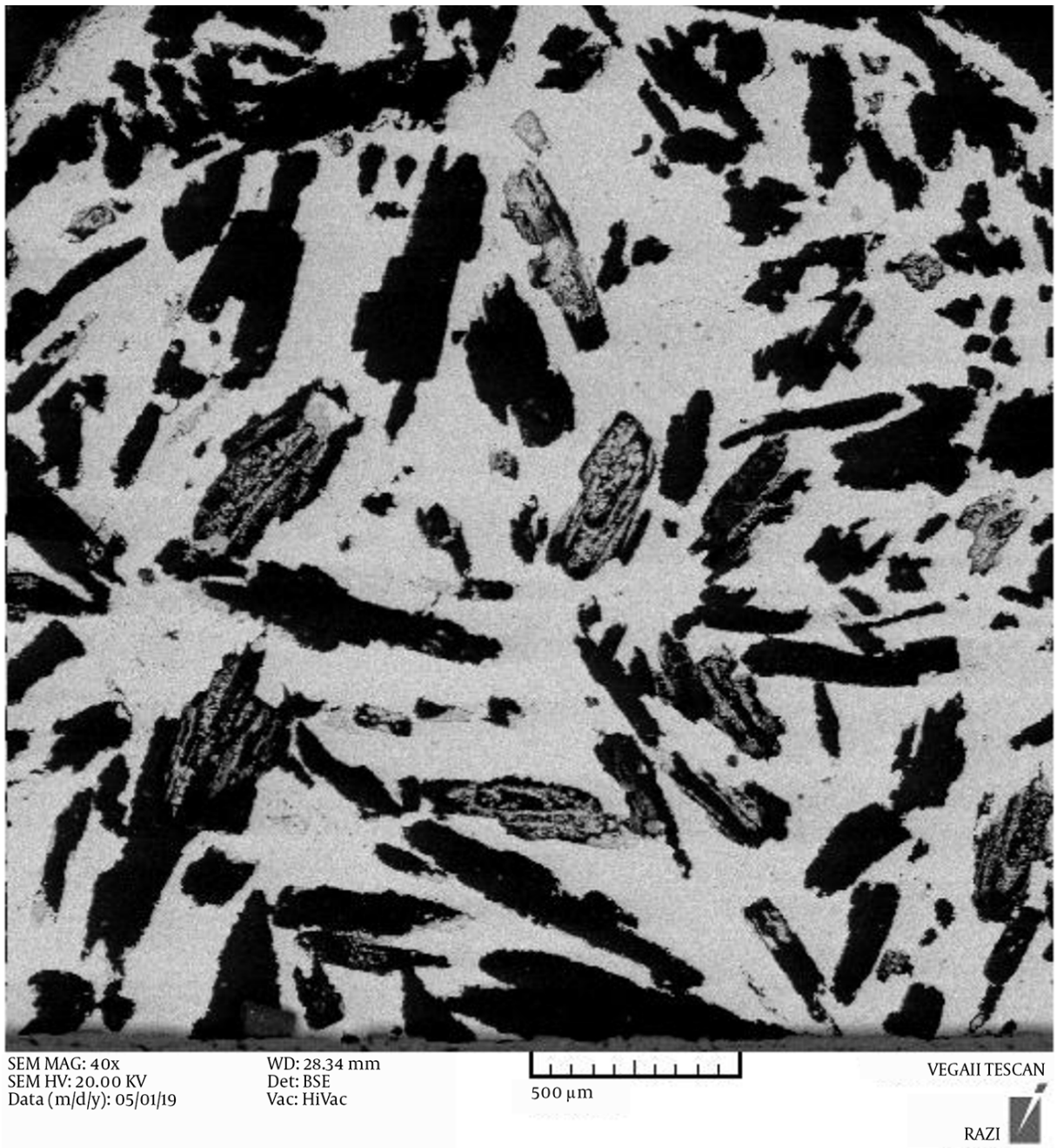

Figure 1. SEM image of the specimens fabricated by acicular urea space holder with a 500 μm magnification

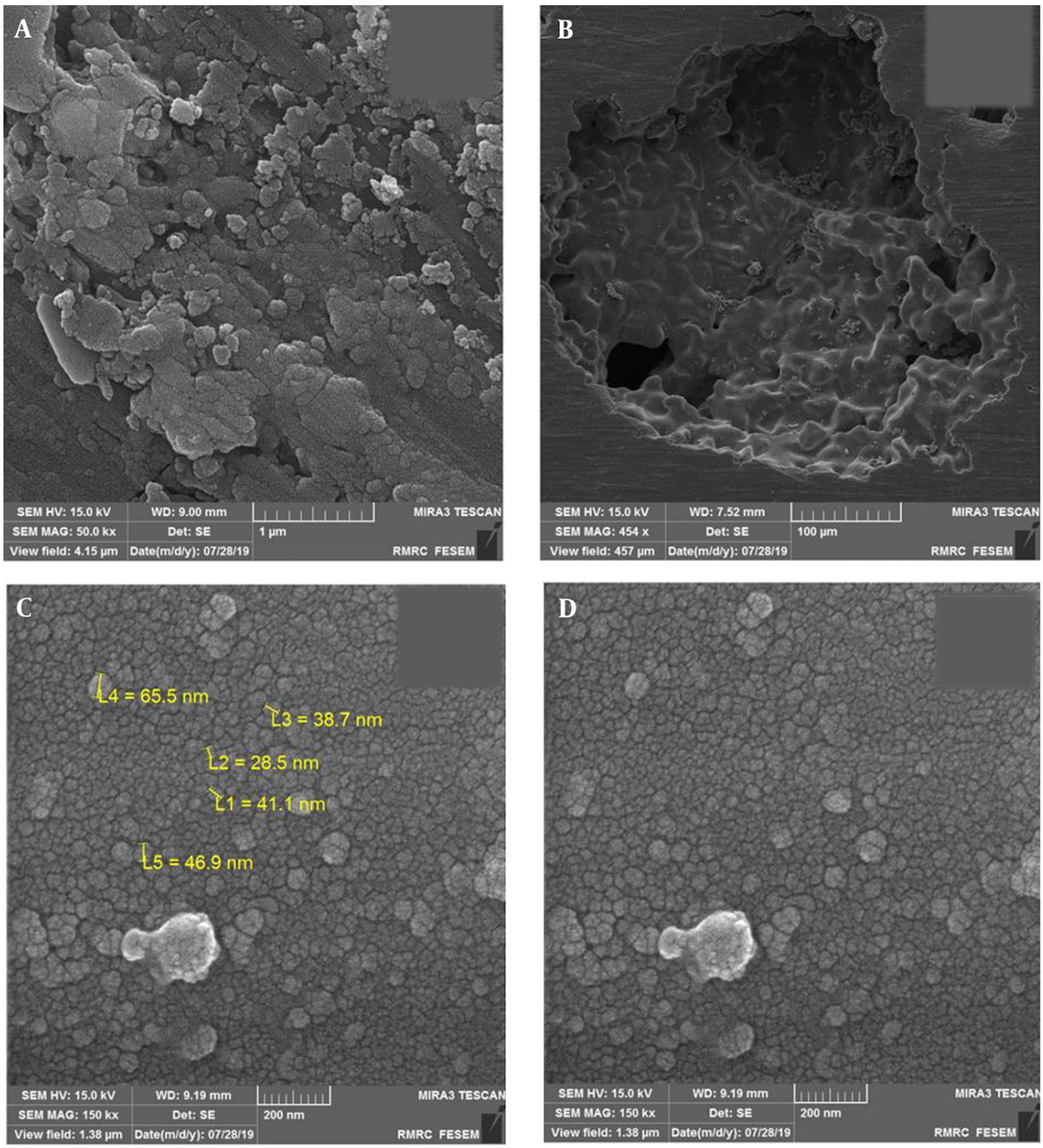

Figure 2. FESEM images of the surface and inside of the sputtering-coated titanium foam; (A) a macropore with a magnification of 500 μm, (B) inside a macropore with a magnification of 1 μm, and (C) and (D) titanium foam surface with a magnification of 200 μm

found in the structure after fabricating porous titanium through powder metallurgy and coating. Considering that the specimens were not oxidized during sintering, higher mechanical properties than scaffolds would be obtained since a powder is better sintered and provides greater mechanical properties (20).

According to Figure 3, the elements of the surface included Ti and O. This suggests a TiO_2 layer on the porous titanium surface after the sputtering process.

4.3. Phase Analysis

TiO_2 has three major phases: (1) anatase, (2) rutile, and (3) brookite. The formation of these three structures is strongly dependent on the temperature (21). Anatase has been reported to begin forming at nearly 300°C. The formation completes once the temperature rises to 600°C (21). A further rise in the temperature creates rutile. Thus, the crystalline structure of the surface oxide could include anatase, rutile, or combined anatase-rutile phases, depending on the heat treatment temperature. However, the formation temperature is dependent on a number of factors, such as the fabrication technique and particle size (21).

Figure 4 plots the XRD patterns of the titanium foam surface and TiO_2-coated titanium surface. As can be seen, the XRD pattern of the coated surface shows peaks for the titanium substrate and TiO_2 layer with a crystalline anatase phase. Since reactions occur at high rates in sputtering, sputtered surface oxide structures are typically amorphous (22). Such structures become crystalline at nearly 300°C. The present study subjected the sputtered surface oxide layer to heat treatment at 480°C for 2 h. According to Figure 4 (b), at $1/2\theta = 25°$, the amorphous phase transformed into a crystalline anatase phase at this temperature. A number of studies reported that anatase is more beneficial than rutile for bone growth since it has higher lattice consistency with hydroxyapatite (23).

4.4. Cell Attachment and Morphology

Figure 5 depicts the SEM-obtained attachment, proliferation, and morphology of MG-63 cells on the specimens within a time interval of 24 h after the culture. As can be seen, the cells highly propagated on the surfaces of both coated and uncoated specimens and adhered to the substrate by attachment protein secretion. However, the proliferation and attachment of cells on the coated surface were found to be much higher than on the uncoated specimen. The proliferation of cells on the coated surface significantly covered the entire surface through pseudopods, while there are areas without cells on the uncoated titanium foam. This suggests that the coating increased the biocompatibility of the substrate (24). Roughness and high surface area provided by the nanostructured coated specimens suggest applicable states for interlocking with bone cells and enhance the bone fixation with the implant (21). Nanostructures offer more appropriate sites compared to pores and surfaces without nanostructure. These nanostructure coatings will increase the adhesion sites to the integrins, adsorb proteins, and facilitate identification of the absorbed proteins on the surface by the integrins (19). These results confirm that nanostructure coatings as a nanoarchitecture parameter plays a crucial role in stages of cell attachment and growth in porous Ti scaffolds.

4.5. Cytotoxicity and Biocompatibility Study

The MTT test was performed to quantify the proliferation of cells on the uncoated and coated surfaces. Figure 6 compares cell survival between the specimens in time intervals of 3 and 7 days after the culture. The MTT results indicated cell growth and proliferation on the surfaces. As can be seen, the survival of MG-63 cells increased from 101.87% on the uncoated surface to 109.27% on the nanostructured TiO_2-coated surface on day 7. The increase in cell viability of the TiO_2-coated specimen compared to the uncoated surface and control samples was significant ($P < 0.05$). Thus, a thin nanostructured TiO_2 coating implemented by magnetron sputtering can be used to effectively coat orthopedic implants. This proper behavior could be attributed to (a) nanostructured TiO_2 thin layer which is like nanosized human tissues, and (b) fully porous structure that provides high specific surface (11).

5. Conclusions

The present study fabricated titanium foam using powder metallurgy and urea as the space holder. A nanostructured thin TiO_2 layer was employed to coat the titanium substrate using magnetron sputtering. A non-cracked, continuous, and uniform coating formed on both the foam surface and on the inner walls of macropores. The TiO_2 coating has a nano-scale structure, and no unwanted compounds formed with TiO_2. The in vitro results indicated that the cells cultured on the coated surface had higher proliferation and induced more pseudopods than those cultured on the uncoated surface. The quantitative investigation of cell proliferation demonstrated that the coating enhanced cell proliferation. The improved biocompatibility, attachment, and growth, and proliferation of osteoblasts on the TiO_2-coated surface demonstrated that TiO_2 coatings could be an efficient and effective method in bone implant applications.

A

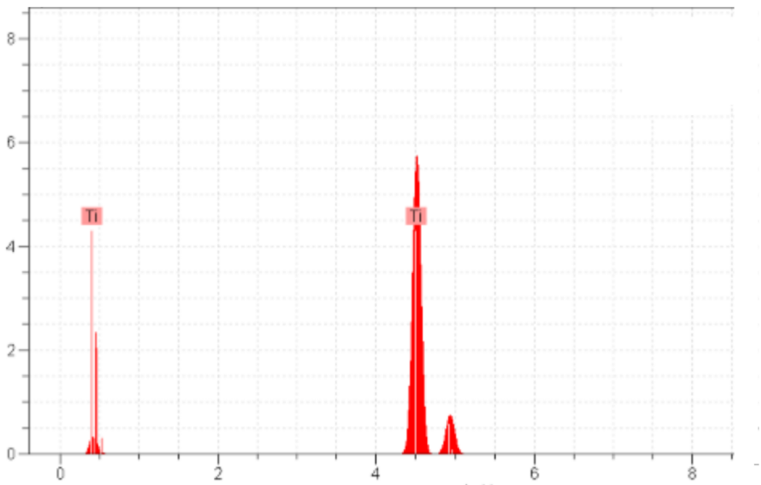

Element	Series	unn. C [wt %]	norm. C [wt%]	Atom. C [at%]
Ti	K series	95.07	100.00	100.00
		Total: 95.1 %		

B

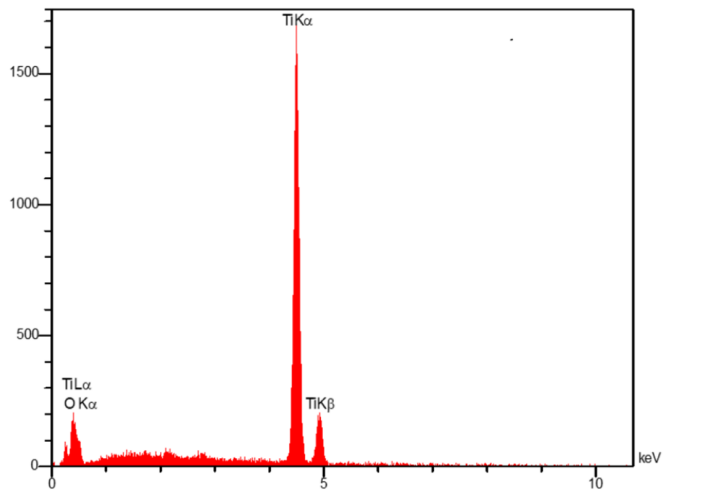

Elt	Line	Int	Error	K	Kr	W%	A%
O	Ka	40.1	18.7121	0.0279	0.0222	18.90	41.10
Ti	Ka	1561.3	1.0765	0.9721	0.7739	81.10	58.90
				1.0000	0.7961	100.00	100.00

Figure 3. EDS results of the porous titanium surface (A) before and (B) after coating with nanostructured TiO_2 through sputtering

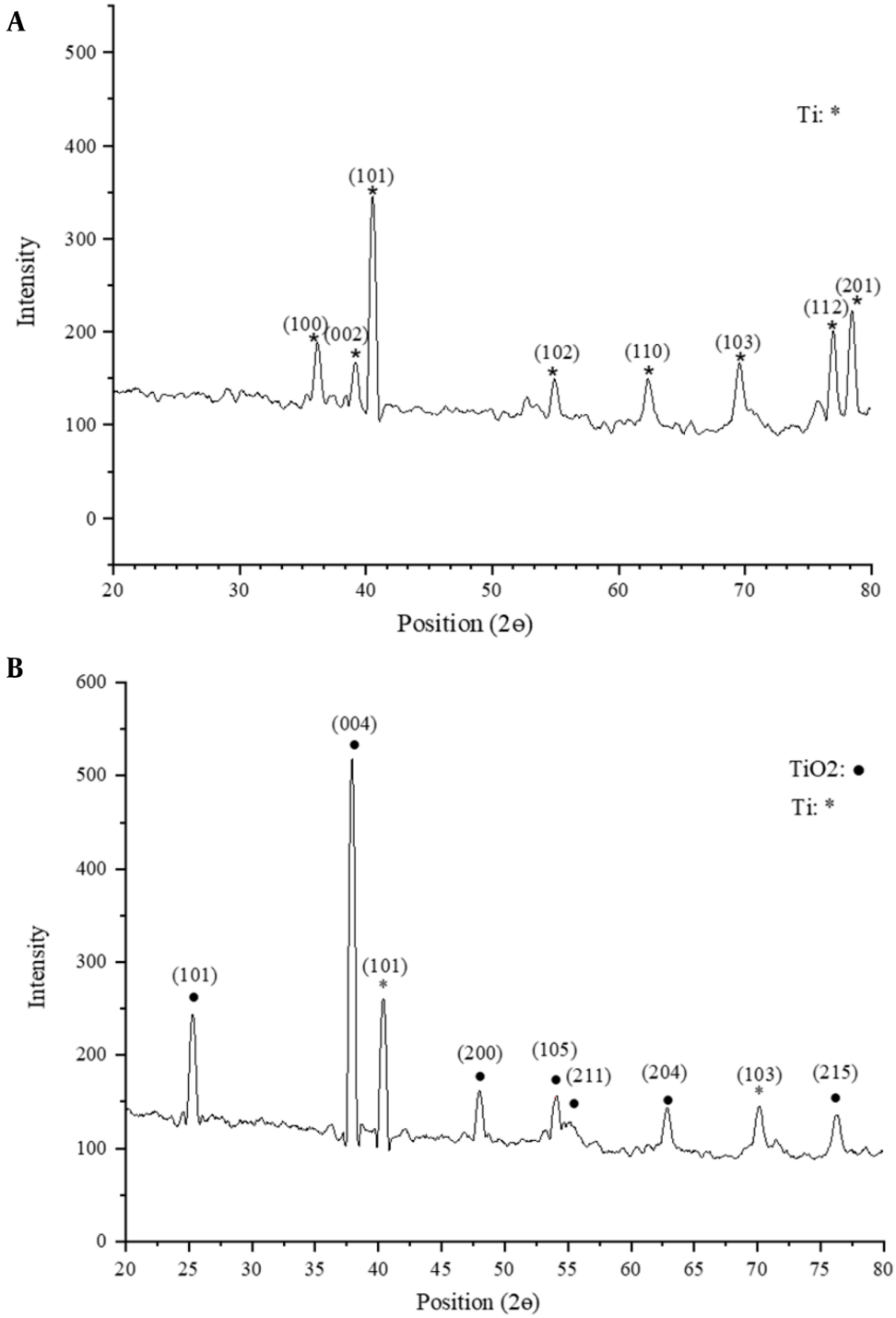

Figure 4. XRD pattern of the (A) uncoated and (B) coated porous titanium surface

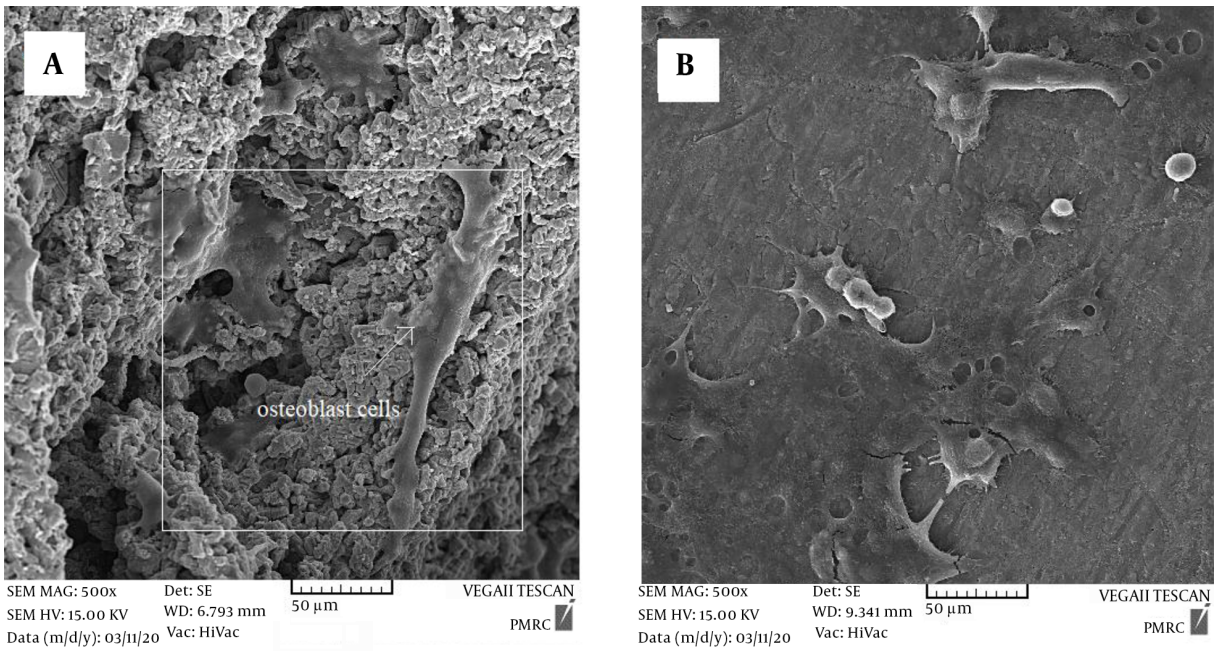

Figure 5. FESEM images of MG-63 cells on (A) uncoated and (B) coated surfaces

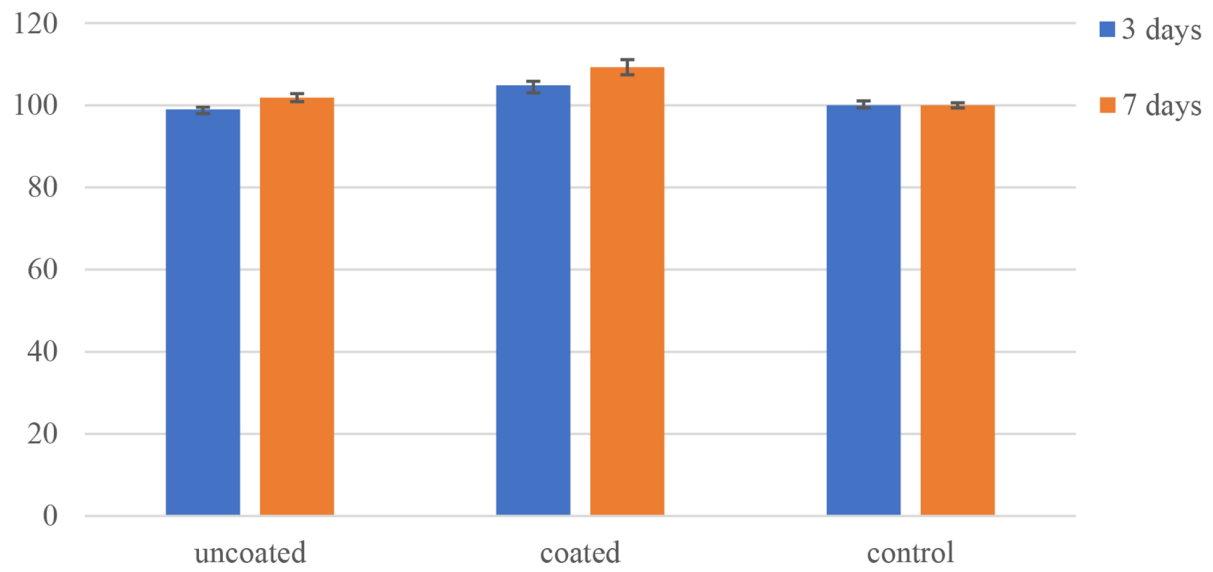

Figure 6. Activity/proliferation of MG-63 cells on the control, coated, and uncoated titanium surfaces

Footnotes

Authors' Contribution: Study concept and design: S.K.S, and R.H..; analysis and interpretation of data: R.H., drafting of the manuscript: R.H.; critical revision of the manuscript for important intellectual content: N.H. and S.K.S; statistical analysis: R.H.

Conflict of Interests: The authors declare that they have no known competing financial interests or personal relationships that could have appeared to influence the work reported in this paper.

Data Reproducibility: The data presented in this study are openly available in one of the repositories or will be available on request from the corresponding author by this journal representative at any time during submission or after publication. Otherwise, all consequences of possible withdrawal or future retraction will be with the corresponding author.

Funding/Support: The authors acknowledge the Iran National Science Foundation for general support and the Advanced Bio-nano Laboratory of the Sharif University of Technology to obtain the experimental work.

References

1. Lascano S, Arévalo C, Montealegre-Melendez I, Muñoz S, Rodriguez-Ortiz JA, Trueba P, et al. Porous titanium for biomedical applications: Evaluation of the conventional powder metallurgy frontier and space-holder technique. *Appl Sci*. 2019;**9**(5):982.
2. Dezfuli SN, Sadrnezhaad SK, Shokrgozar MA, Bonakdar S. Fabrication of biocompatible titanium scaffolds using space holder technique. *J Mater Sci Mater Med*. 2012;**23**(10):2483–8. eng. [PubMed: 22736051]. https://doi.org/10.1007/s10856-012-4706-3.
3. Rivard J, Brailovski V, Dubinskiy S, Prokoshkin S. Fabrication, morphology and mechanical properties of Ti and metastable Ti-based alloy foams for biomedical applications. *Mater Sci Eng C*. 2014;**45**:421–33.
4. Luthringer BJ, Ali F, Akaichi H, Feyerabend F, Ebel T, Willumeit R. Production, characterisation, and cytocompatibility of porous titanium-based particulate scaffolds. *J Mater Sci Mater Med*. 2013;**24**(10):2337–58. eng. [PubMed: 23807315]. https://doi.org/10.1007/s10856-013-4989-z.
5. Ahmadi S, Sadrnezhaad SK. A novel method for production of foamy core@ compact shell Ti6Al4V bone-like composite. *J Alloys Compd*. 2016;**656**:416–22.
6. Cetinel O, Esen Z, Yildirim B. Fabrication, morphology analysis, and mechanical properties of Ti foams manufactured using the space holder method for bone substitute materials. *Metals*. 2019;**9**(3):340.
7. Kashef S, Lin J, Hodgson PD, Yan W. Mechanical properties of titanium foam for biomedical applications. *Int J Mod Phys B*. 2008;**22**(31n32):6155–60.
8. Wang X, Li J, Rui HU, Kou H. Mechanical properties and pore structure deformation behaviour of biomedical porous titanium. *Trans Nonferrous Met Soc China*. 2015;**25**(5):1543–50.
9. Perez RA, Mestres G. Role of pore size and morphology in musculo-skeletal tissue regeneration. *Mater Sci Eng C Mater Biol Appl*. 2016;**61**:922–39. eng. [PubMed: 26838923]. https://doi.org/10.1016/j.msec.2015.12.087.
10. Ahmadi S, Mohammadi I, Sadrnezhaad SK. Hydroxyapatite based and anodic Titania nanotube biocomposite coatings: Fabrication, characterization and electrochemical behavior. *Surf Coat Technol*. 2016;**287**:67–75.
11. Ahmadi S, Riahi Z, Eslami A, Sadrnezhaad SK. Fabrication mechanism of nanostructured HA/TNTs biomedical coatings: An improvement in nanomechanical and in vitro biological responses. *J Mater Sci Mater Med*. 2016;**27**(10):1–15.
12. Chappuis V, Maestre L, Bürki A, Barré S, Buser D, Zysset P, et al. Osseointegration of ultrafine-grained titanium with a hydrophilic nano-patterned surface: an in vivo examination in miniature pigs. *Biomater Sci*. 2018;**6**(9):2448–59. eng. [PubMed: 30065987]. https://doi.org/10.1039/c8bm00671g.
13. Wiatrowski A, Mazur M, Obstarczyk A, Wojcieszak D, Kaczmarek D, Morgiel J, et al. Comparison of the physicochemical properties of TiO2 thin films obtained by magnetron sputtering with continuous and pulsed gas flow. *Coatings*. 2018;**8**(11):412.
14. Poddar NP, Mukherjee S. Characterization of TiO2 thin films deposited by using DC magnetron sputtering. *Carbon Sci Technol*. 2016;**8**:1–8.
15. Chernozem RV, Surmeneva MA, Ignatov VP, Peltek OO, Goncharenko AA, Muslimov AR, et al. Comprehensive Characterization of Titania Nanotubes Fabricated on Ti-Nb Alloys: Surface Topography, Structure, Physicomechanical Behavior, and a Cell Culture Assay. *ACS Biomater Sci Eng*. 2020;**6**(3):1487–99. eng. [PubMed: 33455386]. https://doi.org/10.1021/acsbiomaterials.9b01857.
16. Pansila P, Witit-anun N, Chaiyakun S. Influence of sputtering power on structure and photocatalyst properties of DC magnetron sputtered TiO2 thin film. *Procedia Eng*. 2012;**32**:862–7. https://doi.org/10.1016/j.proeng.2012.02.024.
17. Chen Y, Kent D, Bermingham M, Dehghan-Manshadi A, Wang G, Wen C, et al. Manufacturing of graded titanium scaffolds using a novel space holder technique. *Bioact Mater*. 2017;**2**(4):248–52. https://doi.org/10.1016/j.bioactmat.2017.07.001.
18. Lee B, Lee T, Lee Y, Lee DJ, Jeong J, Yuh J, et al. Space-holder effect on designing pore structure and determining mechanical properties in porous titanium. *Mater Des*. 2014;**57**:712–8. https://doi.org/10.1016/j.matdes.2013.12.078.
19. Rasouli R, Barhoum A, Uludag H. A review of nanostructured surfaces and materials for dental implants: surface coating, patterning and functionalization for improved performance. *Biomater Sci*. 2018;**6**(6):1312–38. eng. [PubMed: 29744496]. https://doi.org/10.1039/c8bm00021b.
20. Fang ZZ, Paramore JD, Sun P, Chandran K, Zhang Y, Xia Y, et al. Powder metallurgy of titanium – past, present, and future. *Int Mater Rev*. 2017;**63**(7):407–59. https://doi.org/10.1080/09506608.2017.1366003.
21. Karazisis D, Petronis S, Agheli H, Emanuelsson L, Norlindh B, Johansson A, et al. The influence of controlled surface nanotopography on the early biological events of osseointegration. *Acta Biomater*. 2017;**53**:559–71. https://doi.org/10.1016/j.actbio.2017.02.026.
22. Valencia-Alvarado R, de la Piedad-Beneitez A, López-Callejas R, Mercado-Cabrera A, Peña-Eguiluz R, Muñoz-Castro AE, et al. TiO2 thin and thick films grown on Si/glass by sputtering of titanium targets in an RF inductively coupled plasma. *J Phys Conf Ser*. 2015;**591**. https://doi.org/10.1088/1742-6596/591/1/012042.
23. Fu Q, Rahaman MN, Bal B, Brown RF. In vitro cellular response to hydroxyapatite scaffolds with oriented pore architectures. *Mater Sci Eng C*. 2009;**29**(7):2147–53. https://doi.org/10.1016/j.msec.2009.04.016.
24. Triviño-Bolaños DF, Camargo-Amado RJ. Synthesis and characterization of porous structures of rutile TiO2 /Na0.8Ti4O8/Na2Ti6O13 for biomedical applications. *MethodsX*. 2019;**6**:1114–23. https://doi.org/10.1016/j.mex.2019.04.002.